JACS
JOURNAL OF THE AMERICAN CHEMICAL SOCIETY
Communication
pubs.acs.org/JACS

A Supramolecular Aggregate of Four Exchange-Biased Single-Molecule Magnets

Tu N. Nguyen,[†] Wolfgang Wernsdorfer,[‡] Khalil A. Abboud,[†] and George Christou*,[†]

[†]Department of Chemistry, University of Florida, Gainesville, Florida 32611-7200, United States
[‡]Institut Néel-CNRS, 38042 Grenoble Cedex 9, France

Supporting Information

ABSTRACT: The reaction between 3-phenyl-1,5-bis(pyridin-2-yl)pentane-1,5-dione dioxime ($pdpdH_2$) and triangular $[Mn^{III}_3O(O_2CMe)(py)_3](ClO_4)$ (**1**) affords $[Mn_{12}O_4(O_2CMe)_{12}(pdpd)_6)](ClO_4)_4$ (**3**). Complex **3** has a rectangular shape and consists of four $[Mn^{III}_3O]^{7+}$ triangular units linked covalently by the dioximate ligands into a supramolecular $[Mn_3]_4$ tetramer. Solid-state dc and ac magnetic susceptibility measurements revealed that $[Mn_3]_4$ contains four Mn_3 single-molecule magnets (SMMs), each with an $S = 6$ ground state. Magnetization versus dc-field sweeps on a single crystal gave hysteresis loops below 1 K that exhibited exchange-biased quantum tunneling of magnetization steps, confirming **3** to be a supramolecular aggregate of four weakly exchange-coupled SMM units.

Single-molecule magnets (SMMs) are individual molecules that function as single-domain nanoscale magnetic particles below their blocking temperature, T_B.[1] This behavior arises from the combination of a large-spin (S) ground state and Ising-type magnetoanisotropy (negative zero-field splitting parameter D), which leads to frequency-dependent out-of-phase alternating current (ac) magnetic susceptibility signals and hysteresis in a plot of magnetization versus applied direct current (dc) magnetic field.[1] SMMs have also been shown to display interesting quantum phenomena such as quantum tunneling of magnetization (QTM)[2] and quantum phase interference (QPI).[3] Consequently, they have been proposed as qubits for quantum computation[4] and as components in molecular spintronics devices,[5] which would exploit their quantum-tunneling properties. For such applications, coupling of two or more SMMs to each other or to other components of a device are essential, but the coupling must be very weak in order to maintain the intrinsic single-molecule properties of each SMM. The report of supramolecular C−H···Cl hydrogen-bonded pairs of $S = {}^9/_2$ $[Mn_4O_3Cl_4(O_2CEt)_3(py)_3]$ SMMs demonstrated such coupling for the first time, manifested as exchange-biased QTM steps, quantum-superposition states, and quantum entanglement of the two SMMs.[6,7] Several supramolecular dimers, chains, and 3D networks of weakly coupled SMMs connected by H-bonds have since been reported.[8] The disadvantages of linkage by H-bonds, however, are (i) deaggregation into monomeric units upon dissolution and (ii) major loss of synthetic control, with all the above examples of supramolecular aggregation by H-bonds in fact having been obtained serendipitously. A superior approach is connection of SMMs via covalent bonds. Such covalent linkage of SMMs has already been explored extensively and usually has been found to lead to 1D, 2D, or 3D polymers.[9] The coupling between these SMMs is often (but not always[10]) strong enough to lead to loss of SMM identity, giving 1D single-chain magnets (SCMs) or 2D- or 3D-ordered materials. However, significant progress has been made in covalent linkage of two non-SMM units for quantum-computing applications, such as linking of two Cr_7Ni wheels[11] or of two lanthanide ions,[12] resulting in weak antiferromagnetic (AF) interactions between them.

Our group has therefore initiated a new effort to link two or more Mn SMMs covalently to give nonpolymeric, supramolecular "clusters of SMMs" showing very weak inter-SMM interactions. We herein report a supramolecular aggregate of four Mn_3 SMMs connected by a newly designed dioxime group, 3-phenyl-1,5-bis(pyridin-2-yl)pentane-1,5-dione dioxime ($pdpdH_2$) (Figure 1). The strategy is based on the observation

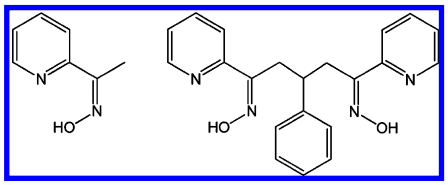

Figure 1. Structures of (left) mpkoH and (right) $pdpdH_2$.

that methyl pyridine-2-yl ketone oxime (mpkoH) reacts with the non-SMM triangular complex $[Mn_3O(O_2CMe)_6(py)_3](ClO_4)$ (**1**) to convert it to the $S = 6$ SMM $[Mn_3O(O_2CMe)_3(mpko)_3](ClO_4)$ (**2**).[13] The new group $pdpdH_2$ consists of two $mpkoH_2$ groups linked by a benzyl unit and is designed to connect two $[Mn_3O]^{7+}$ units. It was synthesized in two steps from 2-acetylpyridine; the intermediate 3-phenyl-1,5-bis(pyridin-2-yl)pentane-1,5-dione was obtained according to a literature method[14] and treated with hydroxylamine to form the crude product. Recrystallization from acetone gave pure $pdpdH_2$ in 55% overall yield.[15]

Reaction of **1** with 1.5 equiv of $pdpdH_2$ in CH_2Cl_2 gave a dark-brown solution. The solution was filtered, and the filtrate was left undisturbed at ambient temperature. X-ray-quality crystals of $[Mn_{12}O_4(O_2CMe)_{12})(pdpd)_6](ClO_4)_4{\cdot}xCH_2Cl_2$ (**3**·$x$$CH_2Cl_2$) slowly formed over 2 days and were collected by filtration; the yield was 35%. Complex **3**·$x$$CH_2Cl_2$

Received: September 16, 2011
Published: December 2, 2011

ACS Publications © 2011 American Chemical Society

dx.doi.org/10.1021/ja2087344 | J. Am. Chem.Soc. 2011, 133, 20688–20691

crystallizes in the monoclinic space group $P2_1/c$.[16] The asymmetric unit consists of two essentially superimposable Mn_{12} cations (one is shown in Figure 2), eight ClO_4^- anions,

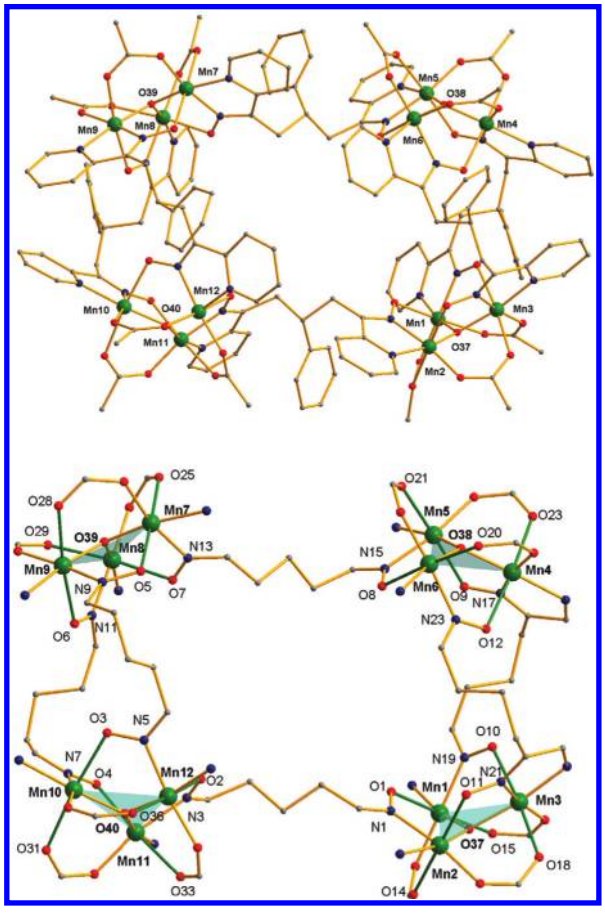

Figure 2. (top) Complete molecular structure of the cation of **3**, with H atoms omitted for clarity. (bottom) Structure of the core, emphasizing the connectivity between the Mn_3 units and showing the Mn_3 planes (green-shaded triangles) and Jahn–Teller axes (green bonds). Color code: Mn, green; N, blue; O, red; C, gray.

and large amounts of disordered CH_2Cl_2 solvent.[16] The Mn_{12} cation consists of four $[Mn_3(\mu_3\text{-O})]^{7+}$ units linked by six $pdpd^{2-}$ groups to give a supramolecular $[Mn_3]_4$ rectangle. One of the two $\eta^1{:}\eta^1{:}\mu$-$MeCO_2^-$ ligands bridging each edge of **1** is replaced by a bridging oximate from a $pdpd^{2-}$ group. Two of the latter bridge to the same neighboring Mn_3 unit, and the third bridges to a different one (Figure 2, bottom). In addition, the $pdpd^{2-}$ pyridyl groups replace the terminal pyridine ligands of **1**. Each of the μ_3-O^{2-} ions lies slightly above its Mn_3 plane ($r \approx 0.3$ Å), as in **2**. Thus, the local structure of each Mn_3 unit of **3** is very similar to that of **2**, comprising a triangular $[Mn_3(\mu_3\text{-O})]^{7+}$ unit whose edges are each bridged by one acetate and one pyridyloximate group, the pyridyl group of which binds terminally to the Mn. Also as in **2**, the three bridging oximate groups are on the same side of the Mn_3 plane, and this is one factor favoring the formation of a molecular tetramer rather than a polymer. In fact, we had anticipated that the product might be an $[Mn_3]_4$ tetrahedron with a bridging $pdpd^{2-}$ on each edge, but the obtained rectangle is also a logical arrangement. The cation has crystallographic C_1 and virtual D_2 symmetry. The Mn^{III} oxidation states were confirmed by bond valence sum calculations,[17] and their Jahn–Teller elongation axes (green bonds in Figure 2, bottom) are aligned in a propeller fashion, again as in **2**. The Mn···Mn separations and Mn–(μ_3-O)–Mn angles in each triangle are slightly different; thus, the triangles are scalene but virtually isosceles within the usual 3σ criterion.[17] Overall, **3** can accurately be described as a tetrameric version of SMM complex **2**, suggesting that each Mn_3 unit of **3** might also be an SMM.

Variable-temperature dc magnetic susceptibility (χ_M) measurements were performed on a polycrystalline sample of $\mathbf{3}{\cdot}2CH_2Cl_2$[16] in an applied field of 1000 G (0.10 T) over the 5.0–300 K temperature range. The sample was restrained in eicosane to prevent torquing. $\chi_M T$ increased from 48.25 cm^3 K mol^{-1} at 300 K to a plateau value of 76.55 cm^3 K mol^{-1} at 20 K and then decreased slightly to 70.62 cm^3 K mol^{-1} at 5.0 K (Figure 3). The 300 K value is much larger than the spin-only

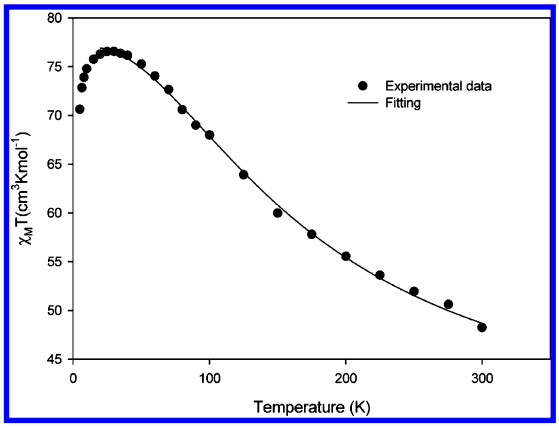

Figure 3. Plot of $\chi_M T$ vs T for $\mathbf{3}{\cdot}2CH_2Cl_2$. The solid line is the fit to the data; see the text for the fit parameters.

($g = 2$) value for 12 Mn^{III} atoms ($\chi_M T = 36$ cm^3 K mol^{-1}), and the peak value at low T is as expected for four noninteracting $S = 6$ units with g slightly less than 2.0 (spin-only $\chi_M T = 84$ cm^3 K mol^{-1}). The decrease in $\chi_M T$ below 20 K is assigned to zero-field splitting (ZFS), Zeeman effects from the applied field, and weak intermolecular interactions. The overall $\chi_M T$ versus T profile is extremely similar to that for complex **2** ($S = 6$), indicating that each of the four Mn_3 units of **3** is also ferromagnetically coupled with an $S = 6$ ground state. The data were fit to the theoretical $\chi_M T$ versus T expression for four independent and equivalent Mn^{III}_3 isosceles triangles per **3**;[13,17] the spin Hamiltonian is given in eq 1:

$$\hat{H} = -2J(\hat{\mathbf{S}}_1{\cdot}\hat{\mathbf{S}}_2 + \hat{\mathbf{S}}_1{\cdot}\hat{\mathbf{S}}_{2'}) - 2J'\hat{\mathbf{S}}_2{\cdot}\hat{\mathbf{S}}_{2'} \quad (1)$$

Only data for $T \geq 20$ K were used because the low-T decrease is due to factors not included in eq 1. The fit gave $J = +16.8(6)$ cm^{-1}, $J' = +1.5(7)$ cm^{-1}, and $g = 1.91(1)$, with temperature-independent paramagnetism (TIP) kept constant at 600×10^{-6} cm^3 mol^{-1}. Since the four Mn_3 units are crystallographically inequivalent, the J and J' are average values, but they are similar to those for **2** and analogues with other carboxylates ($J = +12.1$ to $+18.6$ cm^{-1} and $J' = +1.5$ to $+6.7$ cm^{-1}).

Magnetization (M) data were collected over the 0.1–7 T and 1.8–10 K ranges and are plotted as $M/N\mu_B$ versus H/T in Figure 4, where N is Avogadro's number and μ_B is the Bohr magneton. The data were fit using the program MAGNET by diagonalization of the spin Hamiltonian matrix assuming that only the ground state is populated, incorporating axial anisotropy ($D\hat{S}_z^2$) and Zeeman terms, and employing a full

dx.doi.org/10.1021/ja2087344 | J. Am. Chem.Soc. 2011, 133, 20688–20691

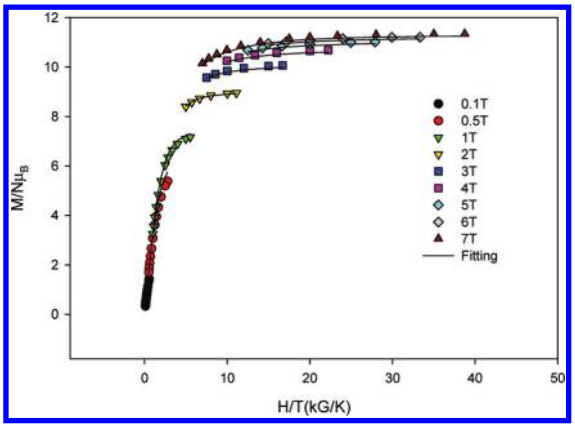

Figure 4. Plot of $M/N\mu_B$ vs H/T per Mn_3 unit of $3{\cdot}2CH_2Cl_2$. The solid lines are the fits to the data; see the text for the fit parameters.

powder average. The spin Hamiltonian is given by eq 2,

$$\hat{H} = D\hat{S}_z^{\,2} + g\mu_B\mu_0\hat{\mathbf{S}}\cdot\mathbf{H} \qquad (2)$$

where D is the axial ZFS parameter, μ_0 is the vacuum permeability, and $\mathbf{H}$ is the applied magnetic field. The fit (solid lines in Figure 4) gave $S = 6$, $D = -0.30(2)$ cm^{-1}, and $g = 1.92(1)$, again very similar to **2** [$S = 6$, $D = -0.34(2)$ cm^{-1}, and $g = 1.92(1)$].[13] The combined dc data thus complement the structural data in supporting the conclusion that complex **3** is a tetramer of four $S = 6$ Mn_3 units like that in **2** and that these units interact with each other only very weakly (too weakly to affect the above fits, which assume noninteracting Mn_3 units).

To probe the SMM properties of $3{\cdot}2CH_2Cl_2$, out-of-phase ac susceptibility (χ_M'') versus T data were collected over the 1.8−15 K range using a 3.5 G ac field oscillating at frequencies of up to 1000 Hz (Figure 5). χ_M'' signals that are tails of peaks lying below 1.8 K

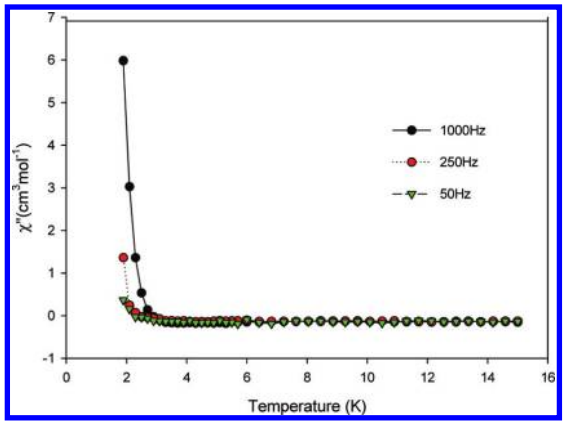

Figure 5. Plots of the out-of-phase ac susceptibility (χ_M'') vs T for $3{\cdot}2CH_2Cl_2$ at the indicated frequencies.

were observed at <3 K, and these suggest that **3** might be a tetramer of SMMs. Therefore, dc magnetization versus field scans on single crystals of $3{\cdot}xCH_2Cl_2$ were carried out on a micro-SQUID.[18] Hysteresis loops were seen below ~1.0 K (Figure 6), and their coercivities increased with decreasing temperature and increasing field sweep rate, as expected for SMMs. We thus conclude that each of the four Mn_3 units in $3{\cdot}xCH_2Cl_2$ is an SMM, as is Mn_3 complex **2** that they closely resemble in structure and magnetic properties.

We now address whether the four Mn_3 SMM units in $3{\cdot}xCH_2Cl_2$ interact weakly with each other. The answer is

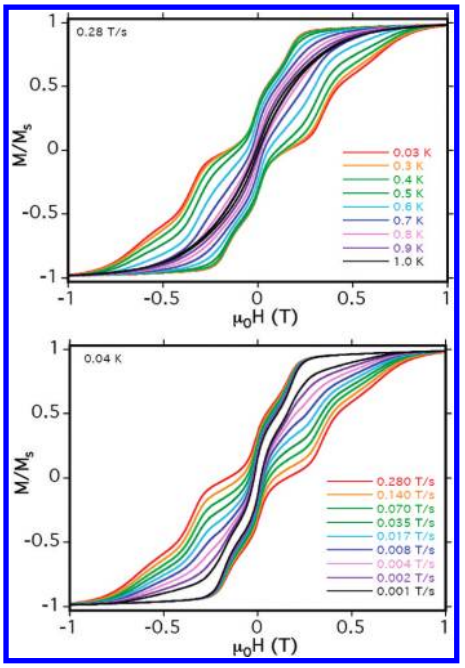

Figure 6. Hysteresis loops in plots of magnetization vs dc field for a single crystal of $3{\cdot}xCH_2Cl_2$ (top) at the indicated temperatures at 0.28 T/s and (bottom) at the indicated field scan rates at 0.04 K. M is normalized to its saturation value, M_S.

clearly yes, because the hysteresis loops show an exchange bias of the QTM steps. The first step in the hysteresis loop of an SMM on scanning from negative to positive fields is normally at zero field. This is where the M_S levels on either side of the anisotropy barrier are in resonance and QTM can occur, reversing the orientation of the magnetization vector. The presence of an AF exchange-coupled neighbor provides a bias field that shifts the resonance tunneling (QTM step) to a new position before zero field. This was first seen for the hydrogen-bonded $[Mn_4]_2$ dimer of $S = {}^9/_2$ SMMs,[6] and a related explanation can be provided for **3**, except that each Mn_3 SMM is now exchange-coupled to two neighboring Mn_3 SMMs. The loops of Figure 6 clearly establish weak AF interactions between the Mn_3 subunits of $3{\cdot}2CH_2Cl_2$. As the field is scanned from −1 T, where the four Mn_3 spin vectors are polarized into the $M_S = -6$ orientation, the first step corresponds to tunneling of a Mn_3 vector from $M_S = -6$ to $M_S = +6$; this occurs at −0.18 T, which thus equals the total bias field from two $M_S = -6$ neighbors. In the format (M_{S1}, M_{S2}, M_{S3}, M_{S4}), where $i = 1$−4 refer to the four Mn_3 SMMs of **3**, the −0.18 T step is the (−6, −6, −6, −6) to (−6, +6, −6, −6) tunneling transition (For clarity, degenerate states such as (−6, −6, +6, −6), (+6, −6, −6, −6), etc., are not listed). Since **3** is a rectangular $[Mn_3]_4$ aggregate, there should be two different inter-Mn_3 interactions, J_1 and J_2, which are likely comparable but not identical in magnitude; the diagonal interaction should be much weaker and is ignored in this discussion. The second step at zero field is assignable to tunneling of molecules with (−6, +6) neighbors, yielding zero bias if $J_1 = J_2$ or a small bias related to $|J_1 - J_2|$ if $J_1 \neq J_2$. The step at zero field is the (−6, +6, −6, −6) to (−6, +6, +6, −6) transition, followed by the possibility of a flip-flop relaxation to the (−6, +6, −6, +6) ground state. A plot of spin-state energy versus applied field showing the avoided level crossings, simulated with $J_1 = J_2 = -0.02$ K and $D = -0.31$ cm^{-1}, is provided in the SI;[17] a detailed analysis will be provided in the full paper on this work. Furthermore, if enough vectors have tunneled to +6 in the first

dx.doi.org/10.1021/ja2087344 | J. Am. Chem.Soc. 2011, 133, 20688−20691

two steps, then a step is expected for Mn_3 vectors tunneling in the presence of a (+6, +6) bias. This should occur at +0.18 T and is indeed seen in Figure 6 (bottom) at 0.001 T/s; at this low scan rate, enough spins have had time to reverse in the first two steps to allow the (+6, +6) situation. At faster scan rates, this step disappears, and even the zero-field step [(−6, +6) bias] becomes smaller because the tunneling probability decreases with increasing scan rate (i.e., fewer molecules are in resonance long enough to tunnel). At high scan rates, at least two new steps appear in the +0.3 to +0.6 T range, also involving $M_S = \pm 5$ levels.[17] The step pattern thus leads to the conclusion that **3** is a supramolecular aggregate of four weakly interacting Mn_3 SMMs, with each Mn_3 coupled to two neighbors.

In summary, a newly designed dioxime has yielded a supramolecular $[Mn_3]_4$ aggregate of four covalently linked SMMs. Each of the Mn_3 subunits of **3** is structurally similar to discrete **2**, and the magnetic properties are therefore also nearly identical. Hysteresis studies showed that each of the four Mn_3 SMMs is weakly coupled to two neighbors, leading to an exchange bias of the QTM steps whose magnitude depends on the spin alignments of these neighbors. We assume at this preliminary stage that the inter-Mn_3 interaction is via superexchange through the bridging ligands, since **2** shows no exchange bias of its QTM steps from intermolecular dipolar interactions. Unfortunately, the QTM steps are relatively broad, possibly as a result of the following: (i) the two Mn_{12} cations in the asymmetric unit have different orientations, and the four Mn_3 planes within each cation are not coplanar (Figure 2, bottom). The applied field will thus be at a range of angles to the easy (z) axes of the eight Mn_3, leading to step broadening; (ii) $J_1 \neq J_2$, and nonzero diagonal interactions within $[Mn_3]_4$ or interactions between separate units will give a range of bias fields for a given (± 6, ± 6) situation. We are thus introducing bulkier carboxylates to isolate Mn_{12} cations more effectively and seeking crystals with all cations parallel. Notably, the covalent linkage within the $[Mn_3]_4$ assembly results in retention of the structure upon dissolution, allowing studies of an exchange-biased system in fluid and frozen solutions for the first time.

In conclusion, **3** confirms the feasibility of covalently connecting multiple Mn_3 SMMs to give a discrete supramolecular "cluster of SMMs" with only weak coupling between them. This should lead to their also being quantum-mechanically coupled, as found for $[Mn_4]_2$ dimers, and represents a step toward the development of a multiqubit system based on SMMs. Such studies are currently in progress, as are additional synthetic efforts to produce other supramolecular aggregates of weakly coupled SMMs.

■ ASSOCIATED CONTENT

Supporting Information

Crystallographic details (CIF), bond valence sums, bond distances and angles, NMR spectra, and magnetism data. This material is available free of charge via the Internet at http://pubs.acs.org.

■ AUTHOR INFORMATION

Corresponding Author

christou@chem.ufl.edu

■ ACKNOWLEDGMENTS

This work was supported by NSF (CHE-0910472). T.N.N. thanks the Vietnam Education Foundation for a fellowship, and W. W. acknowledges the ERC Advanced Grant MolNanoSpin No. 226558.

■ REFERENCES

(1) (a) Sessoli, R.; Gatteschi, D.; Caneschi, A.; Novak, M. A. *Nature* **1993**, *365*, 141. (b) Sessoli, R.; Tsai, H. L.; Schake, A. R.; Wang, S.; Vincent, J. B.; Folting, K.; Gatteschi, D.; Christou, G.; Hendrickson, D. N. *J. Am. Chem. Soc.* **1993**, *115*, 1804. (c) Bagai, R.; Christou, G. *Chem. Soc. Rev.* **2009**, *38*, 1011.

(2) Friedman, J. R.; Sarachik, M. P.; Tejada, J.; Ziolo, R. *Phys. Rev. Lett.* **1996**, *76*, 3830.

(3) Wernsdorfer, W.; Sessoli, R. *Science* **1999**, *284*, 133.

(4) Leuenberger, M. N.; Loss, D. *Nature* **2001**, *410*, 789.

(5) Bogani, L.; Wernsdorfer, W. *Nat. Mater.* **2008**, *7*, 179.

(6) Wernsdorfer, W.; Aliaga-Alcalde, N.; Hendrickson, D. N.; Christou, G. *Nature* **2002**, *416*, 406.

(7) (a) Hill, S.; Edwards, R. S.; Aliaga-Alcalde, N.; Christou, G. *Science* **2003**, *302*, 1015. (b) Tiron, R.; Wernsdorfer, W.; Foguet-Albiol, D.; Aliaga-Alcalde, N.; Christou, G. *Phys. Rev. Lett.* **2003**, *91*, No. 227203.

(8) (a) Tiron, R.; Wernsdorfer, W.; Aliaga-Alcalde, N.; Christou, G. *Phys. Rev. B.* **2003**, *68*, No. 140407. (b) Yang, E.-C.; Wernsdorfer, W.; Hill, S.; Edwards, R. S.; Nakano, M.; Maccagnano, S.; Zakharov, L. N.; Rheingold, A. L.; Christou, G.; Hendrickson, D. N. *Polyhedron* **2003**, *22*, 1727. (c) Wittick, L. M.; Murray, K. S.; Moubaraki, B.; Batten, S. R.; Spiccia, L.; Berry, K. J. *Dalton Trans.* **2004**, 1003. (d) Bagai, R.; Wernsdorfer, W.; Abboud, K. A.; Christou, G. *J. Am. Chem. Soc.* **2007**, *129*, 12918. (e) Inglis, R.; Jones, L. F.; Mason, K.; Collins, A.; Moggach, S. A.; Parsons, S.; Perlepes, S. P.; Wernsdorfer, W.; Brechin, E. K. *Chem.—Eur. J.* **2008**, *14*, 9117. (f) Das, A.; Gieb, K.; Krupskaya, Y.; Demeshko, S.; Dechert, S.; Klingeler, R.; Kataev, V.; Buchner, B.; Muller, P.; Meyer, F. *J. Am. Chem. Soc.* **2011**, *133*, 3433.

(9) (a) Coulon, C.; Miyasaka, H.; Clérac, R. *Struct. Bonding (Berlin)* **2006**, *122*, 163. (b) Xu, H.-B.; Wang, B.-W.; Pan, F.; Wang, Z.-M.; Gao, S. *Angew. Chem., Int. Ed.* **2007**, *46*, 7388. (c) Miyasaka, H.; Yamashita, M. *Dalton Trans.* **2007**, 399. (d) Bogani, L.; Vindigni, A.; Sessoli, R.; Gatteschi, D. *J. Mater. Chem.* **2008**, *18*, 4750. (e) Roubeau, O.; Clérac, R. *Eur. J. Inorg. Chem.* **2008**, 4325.

(10) (a) Miyasaka, H.; Nakata, K.; Lecren, L.; Coulon, C.; Nakazawa, Y.; Fujisaki, T.; Sugiura, K.; Yamashita, M.; Clérac., R. *J. Am. Chem. Soc.* **2006**, *128*, 3770. (b) Langley, S. K.; Chilton, N. F.; Moubaraki, B.; Murray, K. S. *Dalton Trans.* **2011**, *40*, 12201. (c) Shiga, T.; Miyasaka, H.; Yamashita, M.; Morimoto, M.; Irie, M. *Dalton. Trans.* **2011**, *40*, 2275.

(11) Bellini, V.; Lorusso, G.; Candini, A.; Wernsdorfer, W.; Faust, T. B.; Timco, G. A.; Winpenny, R. E. P.; Affronte, M. *Phys. Rev. Lett.* **2011**, *106*, No. 227205.

(12) Aromı, G.; Aguila, D.; Gamez, P.; Luis, F.; Roubeau. O. *Chem. Soc. Rev.* [Online early access]. DOI: 10.1039/c1cs15115k. Published Online: Aug 4, 2011.

(13) Stamatatos, T. C.; Foguet-Albiol, D.; Lee, S.-C.; Stoumpos, C. C.; Raptopoulou, C. P.; Terzis, A.; Wernsdorfer, W.; Hill, S. O.; Perlepes, S. P.; Christou, G. *J. Am. Chem. Soc.* **2007**, *129*, 9484.

(14) Constable, E. C.; Lewis, J.; Liptrot, M. C.; Raithby, P. R. *Inorg. Chim. Acta* **1990**, *178*, 47.

(15) NMR spectra of $pdpdH_2$ are shown in the SI.

(16) Anal. Calcd (Found) for $3{\cdot}2CH_2Cl_2$ ($C_{152}H_{148}Cl_8Mn_{12}N_{24}O_{56}$): C, 43.99 (43.58); H, 3.59 (3.53); N, 8.10 (7.75). The crystal structure shows that two CH_2Cl_2 molecules are encapsulated within the Mn_{12} cation (Figure S3 in the SI).[17] The elemental analysis indicates their retention even after drying in vacuum. Crystal structure data for $3{\cdot}xCH_2Cl_2$: $C_{150}H_{144}Cl_4Mn_{12}N_{24}O_{56}$ (excl. CH_2Cl_2): FW = 3980.05; monoclinic, space group $P2_1/c$; a = 34.190(4) Å, b = 32.890(4) Å, c = 44.013(5) Å, β = 110.320(3)°; V = 46413(9) Å^3, Z = 8; T = 100(2) K; R_1 [$I > 2\sigma(I)$] = 0.0740, wR_2 (F^2, all data) = 0.1886.

(17) See the Supporting Information (SI).

(18) Wernsdorfer, W. *Adv. Chem. Phys.* **2001**, *118*, 99.

■ NOTE ADDED AFTER ASAP PUBLICATION

This paper was published on the Web on December 2, 2011, with an error in eq 1. The corrected version was reposted on December 6, 2011.